EFDA–JET–PR(10)69

P. Mantica, C. Angioni, C. Challis, G. Colyer, L. Frassinetti, N. Hawkes, T. Johnson, M. Tsalas, P.C. deVries, J. Weiland, B. Baiocchi, M.N.A. Beurskens, A.C.A. Figueiredo, C. Giroud, J. Hobirk, E. Joffrin, E. Lerche, V. Naulin, A.G. Peeters, A. Salmi, C. Sozzi, D. Strintzi, G. Staebler, T. Tala, D. Van Eester, T. Versloot and JET EFDA contributors

A Key to Improved Ion Core Confinement in the JET Tokamak: Ion Stiffness Mitigation due to Combined Plasma Rotation and Low Magnetic Shear

A Key to Improved Ion Core Confinement in the JET Tokamak: Ion Stiffness Mitigation due to Combined Plasma Rotation and Low Magnetic Shear

P. Mantica[1], C. Angioni[2], C. Challis[3], G. Colyer[3], L. Frassinetti[4], N. Hawkes[3], T. Johnson[4], M. Tsalas[5], P.C. deVries[6], J. Weiland[7], B. Baiocchi[1, 8], M.N.A. Beurskens[3], A.C.A. Figueiredo[9], C. Giroud[3], J. Hobirk[2], E. Joffrin[10], E. Lerche[11], V. Naulin[12], A.G. Peeters[13], A. Salmi[14], C. Sozzi[1], D. Strintzi[5], G. Staebler[15], T. Tala[16], D. Van Eester[11], T. Versloot[6] and JET EFDA contributors*

JET-EFDA, Culham Science Centre, OX14 3DB, Abingdon, UK

[1]Istituto di Fisica del Plasma 'P.Caldirola', Associazione Euratom-ENEA-CNR, Milano, Italy
[2]Max-Planck-Institut für Plasmaphysik, EURATOM Association, Garching, Germany
[3]EURATOM-CCFE Fusion Association, Culham Science Centre, OX14 3DB, Abingdon, OXON, UK
[4]Association EURATOM - VR, Fusion Plasma Physics, EES, KTH, Stockholm, Sweden
[5]Association EURATOM-Hellenic Republic, Athens, Greece
[6]FOM Institute Rijnhuizen, Association EURATOM-FOM, Nieuwegein, the Netherlands
[7]Chalmers University of Technology and Euratom-VR Association, Göteborg Sweden
[8]Università degli Studi di Milano, Dept. of Physics, Milano, Italy
[9]Associação Euratom-IST, Instituto de Plasmas e Fusão Nuclear, Instituto Superior Técnico, Lisboa, Portugal
[10]Association Euratom-CEA, CEA/IRFM, F-13108 Saint Paul Lez Durance, France
[11]LPP-ERM/KMS, Association Euratom-Belgian State, TEC, B-1000 Brussels, Belgium
[12]Association Euratom-Risø DTU, DK-4000 Roskilde, Denmark
[13]University of Bayreuth, 95440 Bayreuth, Germany
[14]Association EURATOM-Tekes, Aalto University, Department of Applied Physics, Finland
[15]General Atomics, P.O. Box 85608, San Diego, California 92186-5608, USA
[16]Association EURATOM-Tekes, VTT, P.O. Box 1000, FIN-02044 VTT, Finland
** See annex of F. Romanelli et al, "Overview of JET Results", (23rd IAEA Fusion Energy Conference, Daejon, Republic of Korea (2010)).*

Preprint of Paper to be submitted for publication in
Physical Review Letters

ABSTRACT

New transport experiments on JET indicate that ion stiffness mitigation in the core of a rotating plasma as described in [P.Mantica et al., Phys.Rev.Lett. 102, 175002 (2009)] results from the combined effect of high rotational shear and low magnetic shear. The observations have important implications for the understanding of improved ion core confinement in Advanced Tokamak scenarios. Simulations using quasi-linear fluid and gyro-fluid models show features of stiffness mitigation, whilst non-linear gyro-kinetic simulations do not. The JET experiments indicate that AT scenarios in future devices will require sufficient rotational shear and capability of q profile manipulation.

INTRODUCTION

Ion Temperature Gradient (ITG) modes [1-4] are described by theory as featuring a threshold in the inverse ion temperature gradient length ($R/L_{Ti} = R|\nabla T_i|/T_i$, with R the tokamak major radius) above which the ion heat flux (q_i) increases strongly with R/L_{Ti}. This property leads to a level of stiffness of T_i profiles, characterizing how strongly they are tied to the threshold. The role of plasma rotation on threshold and stiffness is of high relevance for predicting the performance of future devices, because the core T_i and fusion power achievable for a given T_i pedestal depend crucially on threshold and stiffness [5] and future devices are expected to exhibit lower rotation than present devices from which scaling laws are derived.

The role of E×B flow shear stabilization [6] has been investigated in non-linear gyro-kinetic and fluid simulations featuring background flow [7-10] and found to result in a threshold up-shift. From these studies the well-known "Waltz" quenching rule has been derived: $\gamma_{E\times B} = \gamma_{noE\times B} - \alpha_E \omega_{E\times B}$ where g is the instability growth rate, $\omega_{E\times B}$ is the flow shearing rate and $\alpha_E \sim 1$ (see [9] for a recent revision). Experimentally, the only study of the impact of rotation on ion threshold and stiffness was performed on JET (R = 2.96m, a = 1m) and reported in [11]. The unexpected result was found that in the plasma core the main effect of rotation is to lower the stiffness rather than increase the threshold, leading to significantly higher values of R/L_{Ti} in rotating plasmas, well above the levels expected by the threshold up-shift foreseen by the Waltz rule.

This Letter presents new experimental results on the combined role of rotation and magnetic shear in lowering ion stiffness, using transport tools such as qi scans and Ti modulation in plasmas with different safety factor (q) profiles and rotation levels. The new empirical hypothesis is proposed that the concomitant presence of high rotational shear and low magnetic shear is the condition for achieving ion stiffness mitigation in tokamaks. The relevance of the results for the improved ion core confinement observed in Hybrid regimes [12] or ion Internal Transport Barriers (ITBs) [13] is examined based on JET data. A comparison to state-of-art theory is finally presented, discussing quasi-linear fluid and gyro-fluid models and non-linear gyro-kinetic simulations.

With reference to the main experiment discussed in [11] [qi scan at $\rho_{tor} = 0.33$ by varying the localization of ion ICH power in (^{3}He)-D minority], reported for sake of comparison in Fig.1a, the

analysis of the data at $\rho_{tor} = 0.64$ (Fig.1b) indicates that at this outer radius the stiffness reduction due to rotation (observed at $\rho_{tor} = 0.33$) is not present. This is confirmed also by T_i modulation data, which yield the slope of the curve as indicated by the two segments. Besides higher values of normalized qi in the outer region, a major difference in plasma parameters between the two regions is the magnetic shear $s = \partial \ln q / \partial \ln r$, with $s>1$ at $\rho_{tor} = 0.64$ whilst $s \sim 0.4$-0.6 at $\rho_{tor} = 0.33$. The rotational shear instead does not show a definite trend with radius. s is determined by EFIT [14] with magnetic, pressure profile and Motional Stark Effect (MSE) or polarimeter data constraints with a statistical error of ±0.05.

ICRH q_i scans at low and high rotation were carried out in discharges with similar parameters as in Fig.1's dataset (L-mode, $B_T = 3.36$T, $I_p = 1.8$MA, $n_{e0} = 3$–$4\ 10^{19}\ m^{-3}$), but in which the q profile, and hence the values of s and s/q, were varied by different methods: Lower Hybrid pre-heat, plasma current (I_p) ramp-up and –down between 1.8 and 3MA within 3.5s, I_p over-shoot [15]. Current relaxation during and after these events provided a range of q profiles, with s between 0.05 and 0.8 ($0.02<s/q<0.5$) at $\rho_{tor} = 0.33$ and between 0.75 and 1.45 ($0.25<s/q<0.7$) at $\rho_{tor} = 0.64$. The aim was to investigate if a low s value is indeed a concomitant requirement for stiffness reduction due to rotation. Ion threshold and stiffness have been identified as in [11] by placing on- and off-axis 3MW of ICRH power in (^{3}He)-D minority at concentrations $n_{^3He}/n_e \sim 6$-8% and measuring R/L_{Ti} with active Charge Exchange Spectroscopy. T_i modulation was performed on top. In the high rotation discharges, up to 11MW of co-injected NBI power was applied. Fig.2a shows as an example the time evolution of the q profile in a low rotation shot with I_p ramp-up and off-axis ICRH. s and s/q at $\rho_{tor} = 0.33$ and 0.64 are shown versus time in Fig.2b. In low NBI discharges, positioning ICRH off-axis implies that the actual R/L_{Ti} at $\rho_{tor} = 0.33$ is a measure of threshold, since q_i is close to zero. Therefore, the time evolution of R/L_{Ti} directly yields the dependence of threshold on s/q, which is expected from linear theory to play a stabilizing effect. Fig.3 shows R/L_{Ti} versus time at $\rho_{tor} = 0.33$ both for the low and high rotation Ip ramp-up shots, and also the prediction for the linear ITG threshold (similar for both shots) using an analytical formula proposed in [16] in the flat density limit

$$R/L_{Ti}^{ITG} = \frac{4}{3}\left(1 + \frac{T_i}{T_e}\right)\cdot\left(1 + 2\ \frac{s}{q}\right) \ for\ \frac{R}{L_n} < 2\left(1 + \frac{T_i}{T_e}\right) \qquad (1)$$

The increase in measured threshold with time following the increase of s/q is in good match with the expected dependence of threshold on s/q from Eq.(1). In spite of such increase in threshold, however, it is remarkable that the time behaviour of R/L_{Ti} in the high rotation shot is opposite, with R/L_{Ti} lying 3 times above threshold in the early phase and dropping to a factor 1.3 of threshold at late times. At low rotation instead also the on-axis ICRH case (not shown, but virtually identical to the off-axis case) due to high stiffness keeps close to threshold with R/L_{Ti} increasing with time. This observation constitutes a beautiful confirmation of the fact that at high rotation the core T_i dynamics is completely dominated by stiffness, and the stiffness reduction is more pronounced when the q profile is flatter (i.e. at early times). At outer radii, where stiffness is high irrespective

of rotation, R/L_{Ti} both at low and high rotation keeps close to 7.5. The transport changes in Fig.3 are accompanied by consistent changes in turbulence measured by correlation reflectometry [17], as discussed in [18].

Similar observations are made with the other schemes for q profile variation. The data are summarized in Fig.4. q_i values are estimated by the PION ICRH code [19]. s is from MSE. Low rotation data show high stiffness irrespective of s, whilst at high rotation the stiffness reduction is larger at low s, allowing R/L_{Ti} up to 10 even at low q_i^{GB}.

Particularly high values of R/L_{Ti} (>10) are achieved in high rotation shots when the $q = 2$ surface is located in a low s region, while the same surface in a higher s region does not lead to evident R/L_{Ti} increase. This evidence ties in well with the fact that the Ti time evolution of high rotation shots shows some abrupt steps down, in addition to the slow trend due to increasing stiffness during current diffusion. The steps are associated with the movement of a low order rational surface from low to higher s. These observations are in line with experimental observations of the beneficial role of low order rationals near $s = 0$ on turbulent transport [20-23], for which a theoretical basis was proposed in [24]. Such effect of rationals appears as a different phenomenon, which adds on top of the stiffness mitigation due to rotation and low s discussed in this Letter. In fact, the effect of rationals is reported both on ions and on electrons [20-23] and also in absence of rotation [20, 23], whilst the stiffness mitigation is only observed on ions and appears strictly linked to rotation. The evidence of ion stiffness reduction due to rotation and low s has profound implications in the interpretation of improved ion core confinement as observed in Hybrid plasmas or ion ITBs, proposing an alternative paradigm to the usual one based on E×B flow shear threshold up-shift. As a matter of fact, both regimes are experimentally observed in conditions of strong rotation and are lost in absence of rotation [23,25]. Also, an important role of q profile manipulation is recognized experimentally [e.g.13,15]. In [26] the role of both rotation and low s was already deduced from JET ITB experimental data. Fig.5 (inset) shows typical JET q profiles in 4 regimes: standard H-mode with fully diffused current, Hybrid, Optimized Shear (OS) and Negative Shear (NS) ITBs. Both Hybrids and ITBs have core regions of very low s. Therefore we have looked for evidence of stiffness mitigation and its impact on confinement in these high performance plasmas. Their position in the q_i^{GB} versus R/L_{Ti} plot at $\rho_{tor} = 0.33$ (Fig.5) shows that the data populate uniformly the region of high R/L^{Ti} and low q_i^{GB}. Some considerations can be made to discriminate if this behaviour is mainly due to stiffness or threshold.

In the core of Hybrids the linear threshold was found between 3.5 and 5 using GS2 [27], well below the actual R/L_{Ti}. The ro-tation is high but smooth, and the flow shearing rate is ~3-4 10^4 s^{-1}, yielding threshold up-shifts ~1. The profiles then lie well above threshold even at small qiGB, indicating low stiffness. This was also confirmed by NBI Ti modulation (not shown). In the outer region the stiffness level is high, with R/L_{Ti} values comparable to those in Fig.1b. R/L_{Ti} versus s at low and high rotation is plotted in Fig.6 from a JET H-mode and Hybrid database. The scatter of points is due to the range in parameters in the database, in first place qi. Still, it is remarkable

that the two clouds clearly separate at low s, with much larger R/L_{Ti} at high rotation. This evidence suggests that stiffness mitigation in the broad low s region is at the origin of the improved core ion confinement. The dependence on s is also one reason (together with different deposition profiles) why not much effect is seen in fully-diffused H-modes when ICRH power is substituted to NBI power, as discussed in [28].

For ITBs, the profiles at trigger yield $\omega_{E\times B} \sim 1\text{-}2\ 10^4\ s^{-1}$, not producing large threshold up-shift. The data lie in Fig.5 in an intermediate region between the rotating shots of Fig.1a and the neoclassical level. In the fully developed ITB however, the ITB itself generates a large localized rotation gradient at ITB location, with values of $\omega_{E\times B} \sim 7\text{-}8\ 10^4\ s^{-1}$, inducing significant threshold up-shifts. It is then difficult to separate the role of threshold and stiffness. Ti modulation has been performed using ^{3}He ICRH modulation. T_i and amplitude profiles with and without ITB are compared in Fig.7a-b for a case of ICRH deposition at ITB location. The ITB acts as a layer of very low incremental diffusivity, with sharp variation of amplitudes, indicating a very low slope of the q_i versus R/L_{Ti} plot. These observations, reported also for electrons in [29], are not consistent with temperatures tight to a high threshold by high stiffness, but rather with either transport above critical with low stiffness, or with subcritical transport. The second hypothesis must be discarded because as in Fig.5 in most cases both ITBs and Hybrids are found well above neoclassical. We conclude that also in ion ITBs the pattern of decreasing stiffness plays a major role, with the threshold up-shift intervening in a non-linear feedback whilst the ITB develops. Such picture for ions is different from that for electrons proposed in [29], with electron ITBs as sub-critical regions in presence of stiff electron transport. The difference is confirmed by the behaviour of electron and ion cold pulses when they meet the ITB propagating from edge (Fig.7c). In the electron case, the cold pulse grows significantly inside the ITB [29], due to re-destabilization of stiff turbulent transport [30]. For ions, with low stiffness in the ITB, the cold pulse growth cannot take place (Fig.7c) but only strong damping is seen.

While in ITB plasmas the H factor ~1.5 is fully due to large core gradients, in the case of Hybrids enhanced pedestal and stabilization of the NTMs also contribute to the H factor. The pedestal has a larger impact on global confinement than the core, due to volume effects, although fusion power benefits in larger measure than confinement from a core improvement. It has been shown statistically over a large database [31] that the contribution of pedestal to total energy is 20–40% both in H-modes and Hybrids and that the H factor up to 1.5 in Hybrids is due in equal parts to core and pedestal improvement, with the core part mainly located in the ion channel. These findings are consistent with our estimate that an increase in R/L_{Ti} from 6 to 10 due to stiffness mitigation in a region up to $\rho_{tor} = 0.6$ at fixed pedestal leads to $\Delta H \sim 0.2$. With regard to NTMs, the experiments show clearly [32] that strong NTM onset leads to an abrupt drop of the H factor to ~1, with a deterioration of T_i profile mainly caused by the braking of plasma rotation. This does not contradict the fact that, when NTM is weak or absent, the core transport dynamics discussed above are at play.

Finally, we address the state of art of theory predictions on the effect of rotation on ion transport. In widely used quasi-linear transport models, such as Weiland [33] or GLF23 [34], which apply

the Waltz rule on a given and restricted choice of spectral wave-numbers, rotation introduces only a (small) threshold up-shift and not a change in slope. The results from the Weiland model for one discharge with $s = 0.57$ are shown in Fig.8a without and with rotation ($\gamma_E = \omega_{E\times B}/c_s/a \sim 0.1$, with $c_s = (T_e/m_i)^{1/2}$). On the other hand, the more recent gyro-fluid TGLF model [35], which makes use of full spectra, indicates a change in slope, in particular in the region of the knee, where the transition between fully developed turbulence and zonal flows quenching takes place. The simulations shown in Fig.8b start from the parameters of one low rotation discharge and scan R/L_{Ti} and R/L_{Te} in a prescribed ratio (taken from experiment) without and with rotation. This effect is possibly due differential suppression of turbulence at various wavelengths, with more suppression of the low stiffer wavelengths. We note that the change in stiffness with rotation is larger at low s, as shown in Fig.8d and in agreement with experiments. The Weiland model has recently been modified to include the dependence of the fastest growing mode number on rotation [36], obtaining (Fig.8a and 8e) results very similar to TGLF.

In order to verify these results, non-linear flux-tube electrostatic gyro-kinetic simulations using GYRO [37] have been made (Fig.8c), with background rotation and electron-ion collisions, for the same parameters as the TGLF simulations. The box size is $62\times222\ \rho_s$ ($\rho_s = (T_e m_i)^{1/2}/eB$) with 64 toroidal modes from $k_y\rho_s = 0.028$ to $k_y\rho_s = 1.78$ and with a minimum $k_x\rho_s = 0.05$ and max $k_x\rho_s = 6.47$ corresponding to a radial resolution $dx/rs = 0.24$. The radial box size corresponds to $\Delta r/a = 0.125$. At low R/L_{Ti}, very large values of $n = 0$ (zonal) electrostatic potential fluctuations are found which strongly reduce the transport and which obliged to perform simulations exceeding 1000 a/cs. The same results are obtained with double radial box size keeping the same radial resolution. We note that runs with reduced number of toroidal modes are not delivering the same strength of zonal flows. With 64 modes, due to the large zonal flows, turbulent transport is rapidly quenched to zero near threshold and there is no hint of stiffness mitigation at high rotation, but basically only a threshold up-shift. Similar results were obtained with GKW [38] as reported in [18] and recently with GS2 on a different case [39-Fig.3a]. Since the mechanisms mentioned above as possible origin of the stiffness reduction in quasi-linear models are also included, and with most resolved treatment, in non-linear gyro-kinetic models, we have to admit that presently the impact of rotation on ion stiffness remains an open issue on the theory side. It deserves further work because, although the region near marginality is numerically challenging, on the other hand it is the operating domain of fusion relevant devices. We also note that none of the models in Fig.8 is in fact reproducing correctly the steep slope of the low rotation data, which may require global gyro-kinetic simulations and turbulence spreading.

In summary, JET experiments show that ion stiffness is reduced by low s and high rotation. This bears the indication that AT scenarios in future devices will require sufficient rotational shear and capability of q profile manipulation.

ACKNOWLEDGEMENTS

This work, supported by the European Communities under the contract of Association EURATOM/ ENEA-CNR, was carried out within EFDA. The views and opinions expressed herein do not necessarily reflect those of the EC. Nonlinear gyro-kinetic simulations were performed on the parallel server Power 6 (Vip) of the IPP-MPG Rechenzentrum Garching, Germany.

REFERENCES

[1]. N. Mattor et al., Physics of Fluids **31**, 1180 (1988)
[2]. F. Romanelli et al., Physics of Fluids B **1**, 1018 (1989)
[3]. J.W. Connor and H.R.Wilson, Plasma Physics and Controlled Fusion **36**, 719 (1994)
[4]. M.Kotschenreuther et al., Physics of Plasmas **2**, 2381 (1995)
[5]. B.Baiocchi et al., submitted to Plasma Physics and Controlled Fusion
[6]. H.Biglari et al., Physics of Fluids B **2**, 2 (1990)
[7]. J. E. Kinsey et al., Physics of Plasmas **12**, 062302 (2005)
[8]. R.E. Waltz et al., Physics of Plasmas **1**, 2229 (1994)
[9]. J. E. Kinsey et al., Physics of Plasmas **14**, 102306 (2007)
[10]. X. Garbet et al., Physics of Plasmas **9**, 3893 (2002)
[11]. P. Mantica et al., Physical Review Letters **102**, 175002 (2009)
[12]. F. Imbeaux et al., Plasma Physics and Controlled Fusion **47**, B179 (2005)
[13]. R.C. Wolf, Plasma Physics and Controlled Fusion **45**, R1 (2003)
[14]. L.L. Lao et al., Fusion Science and Technology. **48**, 968 (2005)
[15]. J. Hobirk et al., submitted to Plasma Physics and Controlled Fusion
[16]. S.C. Guo and F. Romanelli, Physics of Fluids B **5**, 520 (1993)
[17] A.C.A. Figueiredo et al., 36th EPS Conference on Plasma Phys. Sofia, 2009 ECA Vol.33E, P-2.167 (2009)
[18]. P. Mantica et al., Proc. 23rd IAEA Fusion Energy Conference, Daejeon, 2010, (IAEA, Vienna, 2010) EXC/9-2
[19]. L.-G. Eriksson et al., Nuclear Fusion, **33**, 1037 (1993)
[20]. N.J. Lopes Cardozo et al., Plasma Physics and Controlled Fusion **39** B303 (1997)
[21]. M.E. Austin et al., Physics of Plasmas **13**, 082502 (2006)
[22]. E. Joffrin et al., Nuclear Fusion **42**, 235 (2002)
[23]. P.C. de Vries et al, Nuclear Fusion **49**, 075007 (2009)
[24]. R.E. Waltz et al., Physics of Plasmas **13**, 052301 (2006)
[25]. P.A. Politzer et al, Nuclear Fusion **48**, 075001 (2008)
[26]. T. Tala et al., Plasma Physics and Controlled Fusion **43**, 506 (2001)
[27]. M. Kotschenreuther et al., Computer Physics Communications **88**, 128 (1995)
[28]. T.W. Versloot et al., submitted to Nuclear Fusion
[29]. P. Mantica et al., Physical Review Letters **96**, 095002 (2006)
[30]. A. Casati et al., Physics of Plasmas **14**, 092303 (2007)
[31]. L. Frassinetti et al., 37th EPS Conference on Plasma Phys. Dublin, 2010, P-1.1031

[32]. C.D. Challis et al., 36th EPS Conference on Plasma Phys. Sofia, 2009, ECA Vol.33E, P-5.172 (2009)
[33]. J. Weiland, Collective Modes in Inhomogeneous Plasmas (IOP, Bristol, 2000)
[34]. R.E. Waltz et al., Physics of Plasmas, **4**, 2482 (1997)
[35]. G.M. Staebler et al., Physics of Plasmas **12**, 102508 (2005)]
[36]. J. Weiland et al., 38th EPS Conference on Plasma physics, Strasbourg (2011)
[37]. J.Candy and R.E.Waltz, J. Comput. Phys. **186**, 545 (2003)
[38]. A.G. Peeters et al., Computer Physics Communications **180**, 2650(2009)
[39]. E.G. Highcock et al., Physical Review Letters **105**, 215003 (2010)

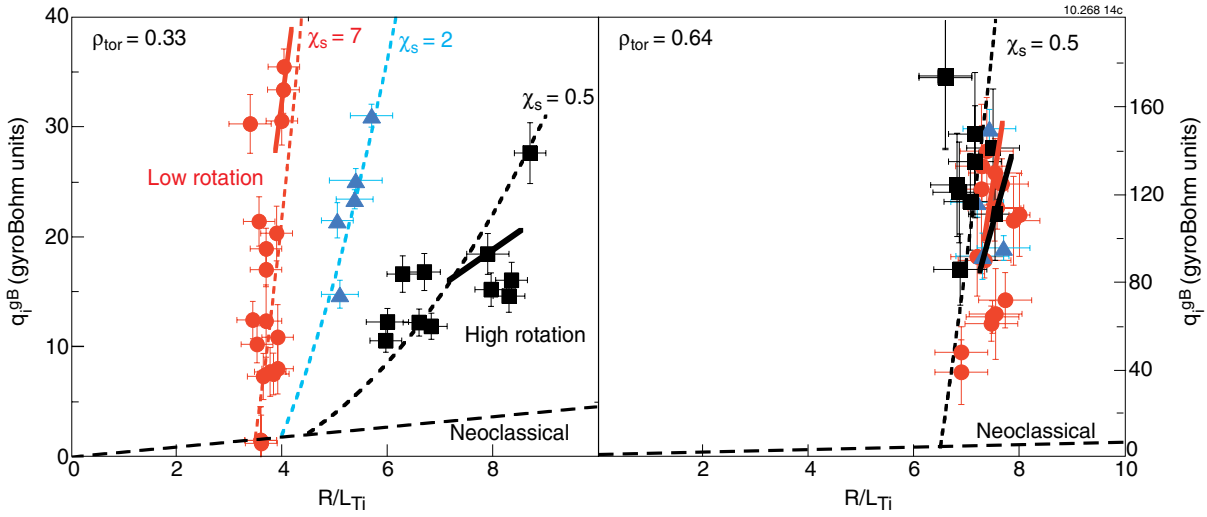

Figure 1:: (colors on-line) q_i^{GB} [=qi/[$(\rho_i/R)^2 v_{ith} n_i T_i$] with $v_{ith}=(T_i/m_i)^{1/2}$, $\rho_i=(T_i m_i)^{1/2}/eB$] versus R/L_{Ti} at (a) $\rho_{tor}=0.33$, (b) $\rho_{tor}=0.64$ for similar plasmas with different levels of rotation. ●:1<ω_0 <2 10^4 rad/s, ▲: 3<ω_0<4 10^4 rad/s, ■: 5<ω_0<6 10^4 rad/s. The dashed black line is indicative of neoclassical transport. The dotted lines represent the Critical Gradient Model (CGM) [11] with different values of χs.

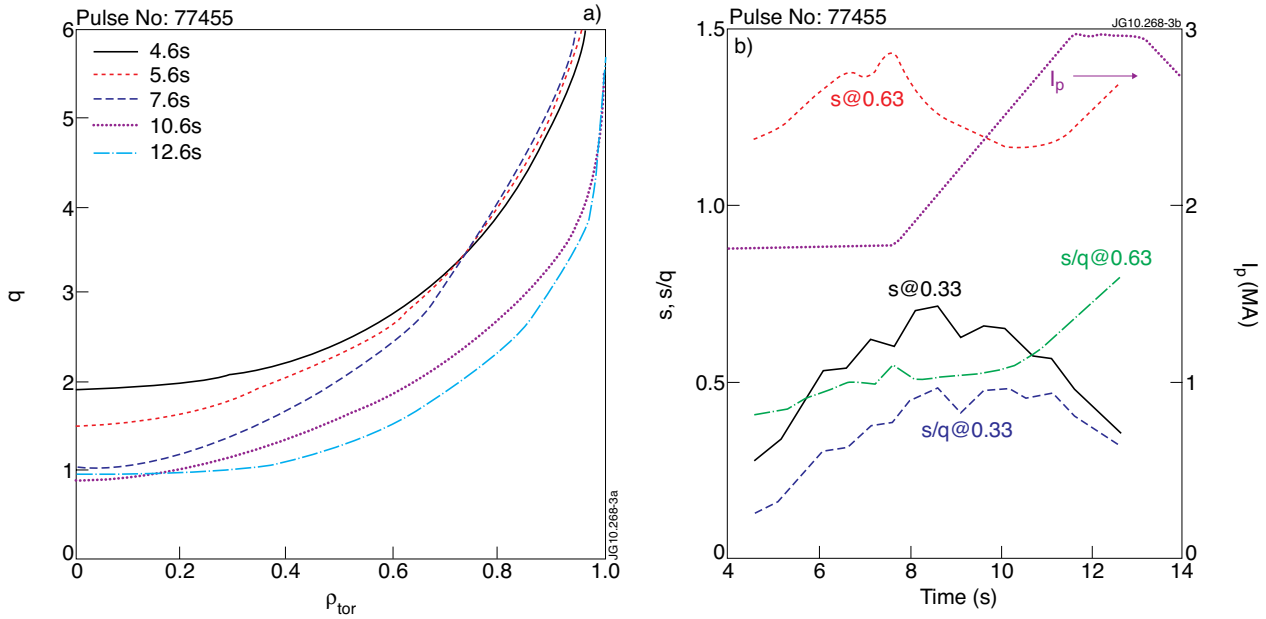

Figure 2: (colors on-line) (a) time evolution of MSE q profile for a low rotation discharge with I_p ram-up; (b) I_p, s, s/q versus time at two radial positions.

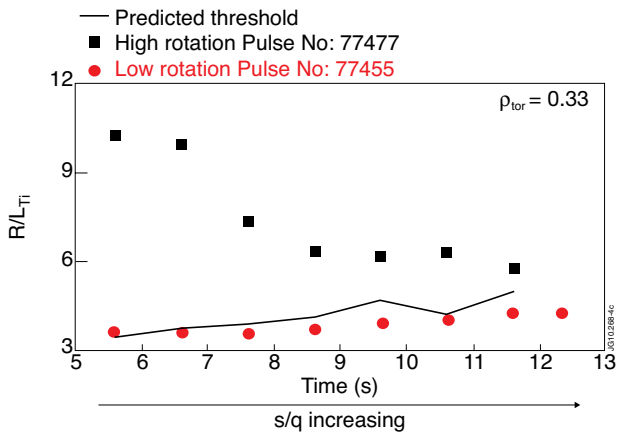

Figure 3: (colors on-line) Experimental R/L_{Ti} at $\rho_{tor} = 0.33$ versus time at low (red circles) and high (black squares) rotation for the I_p ramp-up case, and ITG threshold predicted with Eq.(1).

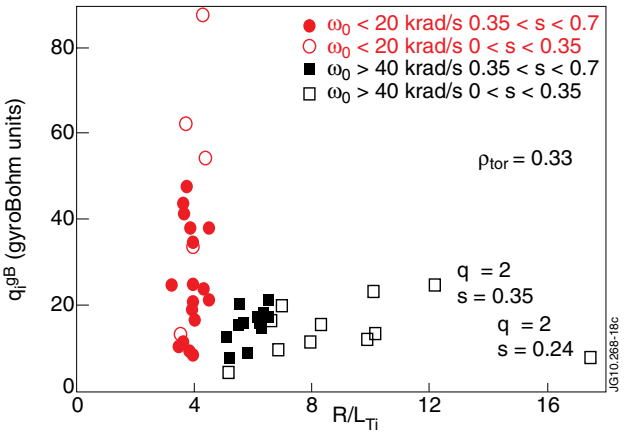

Figure 4: (colors on-line) Gyro-Bohm normalized q_i versus R/L_{Ti} at $\rho_{tor} = 0.33$ for similar plasmas with different rotation and s values.

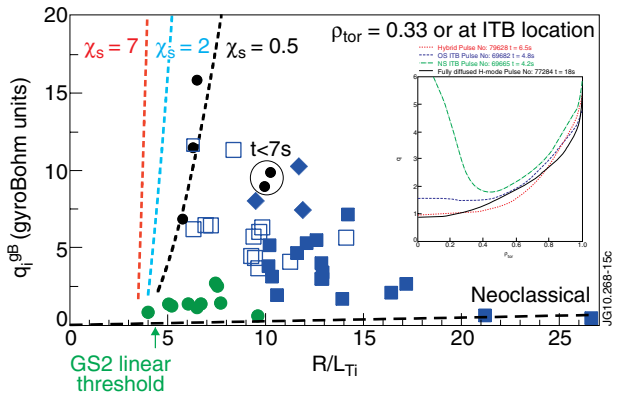

Figure 5: (colors on-line) q_i^{GB} versus R/L_{Ti} at $\rho_{tor} = 0.33$ for a set of Hybrids (green circles), ion ITBs at trigger time (blue open squares) and fully developed (blue full squares, diamonds with large ICRH fraction and reduced rotation). Fig1.a data is indicated by CGM fits. Neoclassical level and GS2 linear threshold for an Hybrid are shown. In the inset q profiles from EFIT-MSE for the 4 scenarios are shown.

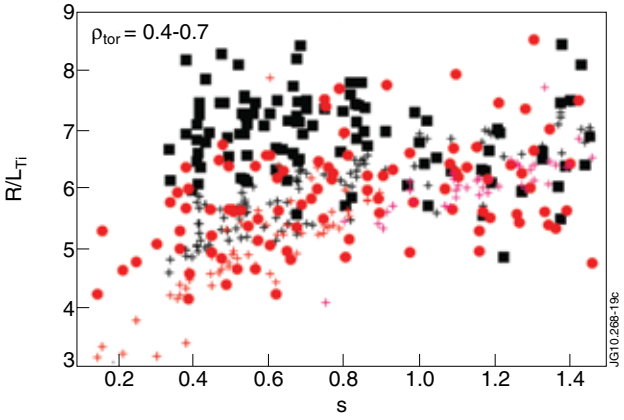

Figure 6: (colors on-line) R/L_{Ti} versus s at $\rho_{tor} = 0.4$-0.7 at low (red circles, $\nabla\omega_t < 50$ krad/(ms)) and high (black squares, $\nabla\omega_t > 130$ krad/(ms))) rotation from a Hybrid and H-mode JET database. s is from EFIT with polarimeter. Crosses are threshold values after Eq.(1)

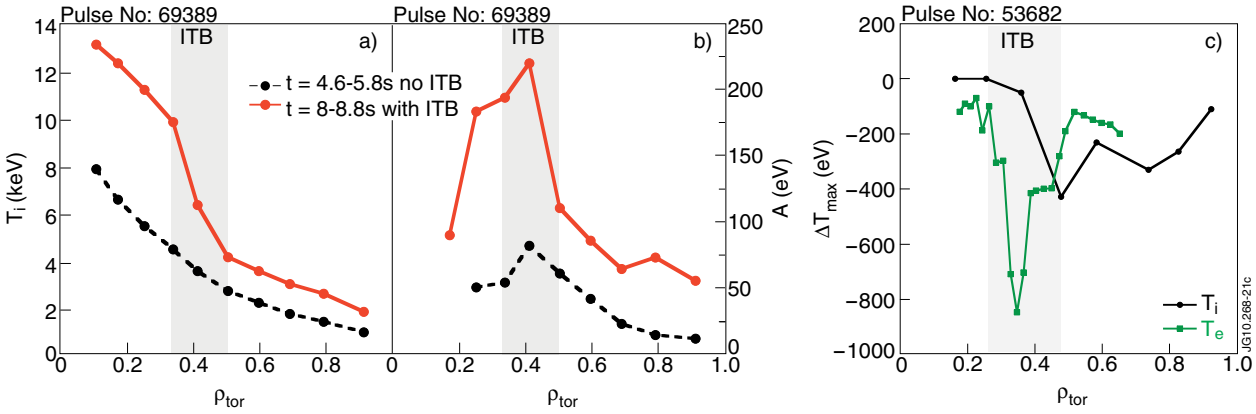

Figure 7: (colors on-line) a) T_i, b) amplitudes for an ITB discharge before trigger (black dashed line) and at full development (red full line). c) Ion and electron cold pulse maximum amplitude.

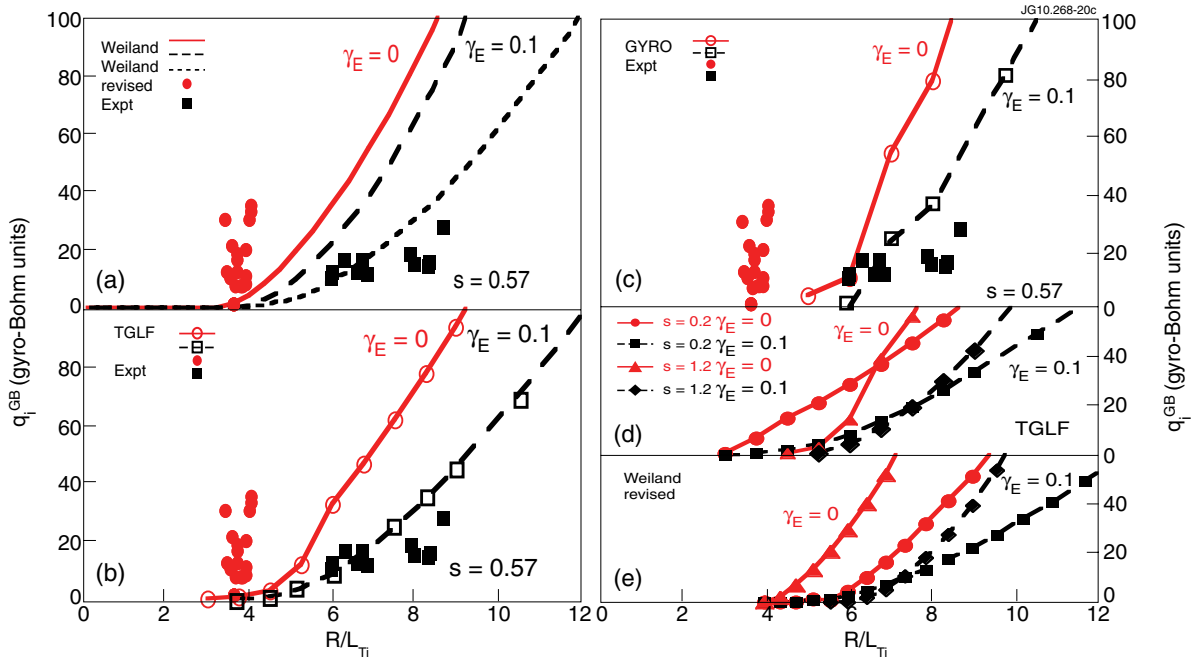

Figure 8: (colors on-line): q_i^{GB} versus R/L_{Ti} at $\rho_{tor} = 0.33$ without and with rotation from a) Weiland, b) TGLF and c) GYRO simulations with $s = 0.57$ compared with the data of Fig.1a. d) TGLF and e) revised Weiland (legend as in d)) simulations with $s = 0.2$ and 1.2.